The Process of Amyloid-like Fibril Formation by Methionine Aminopeptidase from a Hyperthermophile, *Pyrococcus furiosus*†

Katsuhide Yutani,*,‡ Goh Takayama,‡ Shuichiro Goda,‡ Yuriko Yamagata,§ Saori Maki,|| Keiichi Namba,||,⊥ Susumu Tsunasawa,# and Kyoko Ogasahara‡

Institute for Protein Research and Graduate School of Pharmaceutical Sciences, Osaka University, Yamadaoka, Suita, Osaka 565-0871, Japan, Protonic Nano Machine Project, ERATO, JST, 3-4 Hikaridai, Seika 619-0237, Japan, International Institute for Advanced Research, Matsushita Electric Industrial Co., Ltd. 3-4 Hikaridai, Seika 619-0237, Japan, and Gene Analysis Center, Takara Shuzo Co. Ltd., Noji, Kusatsu City, Shiga 520-0055, Japan

Received June 18, 1999; Revised Manuscript Received November 2, 1999

ABSTRACT: Amyloid is associated with serious diseases including Altzheimer's disease and senile-systemic amyloidosis due to misfolded proteins. In the course of study of the denaturation process of methionine aminopeptidase (MAP) from the hyperthermophile *P. furiosus*, we found that MAP forms amyloid-like fibrils, and we then investigated the mechanism of amyloid fibril formation. The kinetic experiments on denaturation monitored by CD at 222 nm indicated that MAP in the presence of 3.37 M GuHCl at pH 3.31 changed to a conformation containing a considerable content of β-sheet structure after the destruction of the α-helical structure. MAP in this β-rich conformation was highly associated, and its stability was remarkably high: the midpoint of the GuHCl denaturation curve was 4.82 M at pH 3.0, and a thermal transition was not observed up to 125 °C by calorimetry. The amyloid-like fibril formation of MAP was confirmed by Congo red staining with a typical peak at 542 nm in the difference spectrum, showing a cross-β X-ray diffraction pattern with a clear sharp reflection at 4.7 Å and a characteristic unbranched fibrillar appearance with a length of about 1000 Å and a diameter of about 70 Å in the electron micrographs. Present results indicate that the amyloid-like form of MAP appears just after the protein is almost completely denatured, and even highly stable proteins can also form amyloid-like conformation under conditions where the denatured state of the protein is abundantly populated.

Amyloidosis is a heterogeneous group of disorders characterized by the accumulation of extracellular deposition of abnormal protein fibrils (*1*). Amyloid is associated with serious diseases including Altzheimer's disease, senile-systemic amyloidosis, and prion-mediated disease, which are called conformational diseases because they are originated from protein misfolding (*2*). Proteins known to form amyloid fibrils in vivo have no homology in their sequences and the three-dimensional structures in their native state forms, but amyloid fibrils have a common core structure (*3*). All amyloid fibrils are long and unbranched with diameters of 60−120 Å (*4*), and they assemble into a cross-β-fiber structure, with β-strands perpendicular and β-sheets parallel to the fiber axis (*5*). X-ray diffraction patterns from amyloid fibrils show simple patterns with 4.7 Å meridional reflections and a broad peak around the 10 Å equatorial region, which are characteristic of a cross-β-structure (*5*).

About 16 different proteins are known to be involved in amyloid diseases (*6*). Colon and Kelly have reported that purified transthyretin is converted into amyloid fibrils through an acid-mediated conformational change, producing an amyloidogenic intermediate that self-assembled into amyloid fibrils (*7*). Following this study starting with Colon and Kelly (*7*), amyloidogenic proteins have been extensively studied from physicochemical points of view (*8*−*21*). It has been reported earlier that a nonamyloidogenic protein, insulin, also could be converted into amyloid (*22, 23*). Recently, Dobson's group has found that two small proteins, the SH3 domain of the p85α subunit of phosphatidylinositol 3-kinase and acylphosphatase, which are not associated with any of the known amyloid diseases, form amyloid fibrils in vitro under acidic conditions (*24*) and in the presence of trifluoroethanol (*25*), respectively. The amyloid fibrils of the acylphosphatase form with a slow transition from the α-helical conformation to one containing a considerable content of β-sheet in a solution containing moderate concentrations of trifluoroethanol. These results suggest that the formation of amyloid fibrils is a common property of proteins and that natural proteins might assemble into such fibrils if appropriate conditions could be found. It is important to elucidate whether amyloid formation is a property common to many proteins and how amyloid fibrils form, to understand the mechanism of the misfolding of proteins and amyloid fibril formation in disease states.

† This work was supported in part by a grant-in-aid for special project research from the Ministry of Education, Science, and Culture of Japan (K.Y.).

* Corresponding author: Institute for Protein Research, Osaka University, Yamadaoka, Suita, Osaka 565-0871, Japan. Telephone: +81-6-6879-8615; Fax: +81-6-6879-8616; E-mail: yutani@protein.osaka-u.ac.jp.

‡ Institute for Protein Research, Osaka University.

§ Graduate School of Pharmaceutical Sciences, Osaka University.

|| Protonic Nano Machine Project, ERATO, JST.

⊥ International Institute for Advanced Research, Matsushita Electric Industrial Co., Ltd.

Gene Analysis Center, Takara Shuzo Co. Ltd.

10.1021/bi991406v CCC: $19.00
Published on Web 02/19/2000

We have investigated the molecular origin of the unusually high stability of hyperthermophile proteins (*26*, *27*). One of them (*26*) is a methionine aminopeptidase (MAP)[1] from a hyperthermophile, *Pyrococcus furiosus*, which catalyzes the cleavage of the N-terminal methionine of proteins. MAP consists of 295 residues (MW = 32 700) and is a monomeric protein under physiological conditions (*26*, *28*). In the course of study of the denaturation process of MAP, we found strange phenomena. Time-dependent conformational changes in MAP, which were induced by concentration jumps of guanidine hydrochloride (GuHCl) from 0 to 3.3 M at acidic pH, were followed by monitoring the CD values at 222 nm. Although the negative CD values were expected to decrease, they increased with time. This indicates the formation of secondary structures due to the concentration jumps of GuHCl. As described in the text, these phenomena were caused by formation of the β-structure after denaturation of MAP. This β-structure formation could be associated with the formation of amyloid-like fibrils, based on the three criteria of amyloid: staining with Congo red, unbranched fibrillar appearance in electron micrographs, and a cross-β X-ray diffraction pattern. In this paper, the amyloid-like fibril formation of MAP from *P. furiosus* and the mechanism of its formation will be discussed.

EXPERIMENTAL PROCEDURES

Protein Expression and Purification. MAP was expressed in the *E. coli* strain JM109/pMap8 by cloning the MAP gene from *P. furiosus* (*28*). The *E. coli* strain JM109/pMap8 was routinely grown in 15 L of LB medium supplemented with ampicillin in 100 mg/L of culture medium at 37 °C for 20 h with shaking.

MAP was purified as previously described (*26*). The final step in the purification was done by anion ion exchange chromatography with a linear gradient of 30−240 mM potassium phosphate buffer (pH 7.0) using SP Sepharose10/26 (Pharmacia). Purified MAP with a single band on SDS−PAGE was stored at − 20 °C.

The protein concentration of MAP was estimated from the absorbance at the maximum wavelength of 278.5 nm, using $E^{1\%} = 9.63$ with a cell having a 1 cm light path length (*26*).

CD Spectra. Far- and near-UV CD spectra were recorded on a Jasco J-720 spectropolarimeter equipped with an NEC personal computer. Spectra were accumulated by scanning 16 times at a scan rate of 20 nm/min, using a time constant of 0.25 s. The light path lengths of the cells used were 0.1 mm in the far-UV region and 10 mm in the near-UV region. The protein concentrations under measurements were 0.9−1.3 mg/mL. For calculation of the mean residue ellipticity, [θ], the mean residue weight was taken as 111.3. All of the CD measurements were carried out at 25 °C.

Denaturation Experiments by GuHCl. The reactions of denaturation were initiated by concentration jumps of GuHCl in the acidic region at 25 °C, and the subsequent time-dependent changes in peptidyl CD at 222 nm were monitored using a Jasco J-720 spectropolarimeter. One volume of the native protein was rapidly added manually to 10 volumes of GuHCl solution of various concentrations in the cell with a 10 mm light path length under stirring using a 4-fin spinning mixer with a magnetic stirrer, and the peptidyl CD was recorded as a function of time. The dead time for this procedure was 1 s. Prior to kinetic experiments, the MAP used was dialyzed in 50 mM Gly buffer at pH 3.0 overnight. Protein concentrations were 0.009−0.012 mg/mL under CD measurements.

For an MAP solution incubated in various GuHCl concentrations at different pHs for a long period of more than 1 day, CD spectra were measured at protein concentrations of 0.09−0.12 mg/mL using a cell with a 1 mm light path length.

Guanidine hydrochloride (GuHCl) (specially prepared reagent grade) from Nacalai Tesque (Kyoto, Japan) was used without further purification. The GuHCl concentrations were determined by refraction using an Abbe refractometer (Atago 3T) at 20 °C. Other chemicals were reagent grade.

Differential Scanning Calorimetry. The DSC measurements were performed at a scanning rate of 1 K/min under a pressure of 30 psi using a Micro Cal VP-DSC. Prior to the measurements, the MAP solution in the presence of GuHCl was dialyzed overnight against a buffer solution containing GuHCl at 4 °C. Samples were filtered through a 0.22 μm pore size filter and degassed under vacuum. The pH value of the sample was measured after DSC measurements.

Analytical Ultracentrifugation. Analytical ultracentrifugation was carried out with a Beckmann Optima model XL-A. Sedimentation equilibrium experiments were performed at 20 °C at a speed of 5000 rpm for the samples in the presence of GuHCl and at 12 000 rpm for the sample in the absence of GuHCl. It took 2 days to attain an equilibrium state in the presence of GuHCl. Prior to the measurements, the protein solutions were dialyzed overnight against 50 mM Gly-HCl buffer containing various concentrations of GuHCl at pH 3.0 and at 4 °C. The experiments at three different protein concentrations between 1.0 and 0.5 mg/mL were run in Beckman 4-sector cells. The partial specific volume of MAP was assumed to be 0.755 cm^3/g from the amino acid composition (*29*).

Congo Red Staining. The binding test of the associated form of MAP containing a considerable content of β-sheet (Am-form) with Congo red was performed according to the method reported by Klunk et al. (*30*). Congo red (Wako Pure Chemicals Industries, Ltd.) solution was freshly prepared and filtered twice through a filter of 0.22 μm pore size before use. The final concentration of Congo red in the test solution was about 7 μM in 5 mM potassium phosphate of pH 7.4 containing 0.15 M NaCl. A Nikon polarized microscope (Optiphot-Pol) was used for birefringence measurements.

Electron Microscopy. The supernatant and precipitate of the Am-form of MAP were applied to carbon-coated copper grids, blotted, washed, negatively-stained with 2% uranyl acetate (w/v), air-dried, and then examined with a JEOL JEM 1010 transmission electron microscope operating at an accelerating voltage of 100 kV.

X-ray Diffraction. The precipitate of the Am-form of MAP was put into a capillary of 0.7 mm diameter. X-ray diffraction experiments were carried out using a Rigaku rotating-anode X-ray generator, RU-300 (Tokyo), operated at 40 kV and

[1] Abbreviations: MAP, methionine aminopeptidase from *Pyrococcus furiosus*; CD, circular dichroism; DSC, differential scanning calorimetry; GuHCl, guanidine hydrochloride; Am-form of MAP, the association form of MAP containing a considerable content of β-sheet.

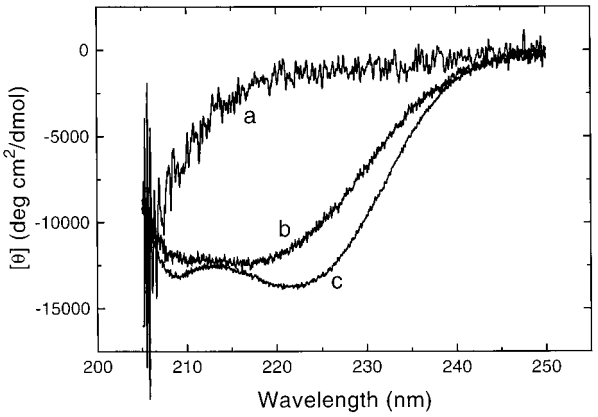

FIGURE 1: CD spectra in the far-UV region of MAP in the presence of different concentrations of GuHCl at 25 °C. Spectra for MAP in 5.90 M GuHCl at pH 2.89 (a), 3.27 M GuHCl at pH 2.91 (b), and 0 M GuHCl at pH 3.04 (c) in 50 mM Gly-HCl buffer were measured after incubation under each condition for 24 h at 25 °C.

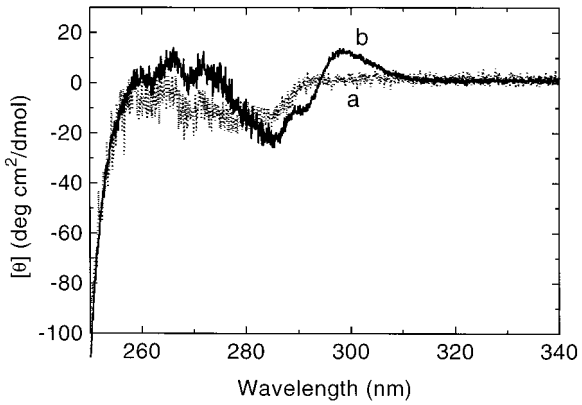

FIGURE 2: CD spectra in the near-UV region of MAP in 3.29 M GuHCl at pH 3.56 (a) and in 0 M GuHCl at pH 3.02 (b). The spectra were measured after 24 h incubation at 25 °C.

200 mA ($\lambda = 1.5418$ Å). The specimen-to-film distance and the exposure time were 100 mm and 10 h, respectively. X-ray diffraction patterns were recorded on an imaging plate detector R-AXIS IIC.

RESULTS

Denaturation Process of MAP by GuHCl. The far- and near-UV CD spectra of MAP from *P. furiosus* in the absence of GuHCl at pH 3.0 as shown in Figure 1 (c) and Figure 2 (b), respectively, were identical to those in the native state at pH 7.0 (*26*). This suggests that the conformation of MAP in the absence of GuHCl at pH 3.0 is still in the native state. This was also confirmed by calorimetry as shown below [Figure 5(a),(b)]. The far-UV CD spectrum in 5.9 M GuHCl at pH 2.9 [Figure 1(a)] was a typical feature of the denatured state of a protein.

The denaturation reaction of the MAP was induced by GuHCl concentration jumps from 0 M to various concentrations at 25 °C, and subsequent time-dependent changes in the CD at 222 nm were recorded. The decreases in the negative CD values which reflect the disruption of secondary structures with time were observed in the neutral pH region (data not shown). However, when the GuHCl concentration jumped from 0 to 3.65 M at pH 2.9, the negative CD values at 222 nm increased from the denatured value to the native

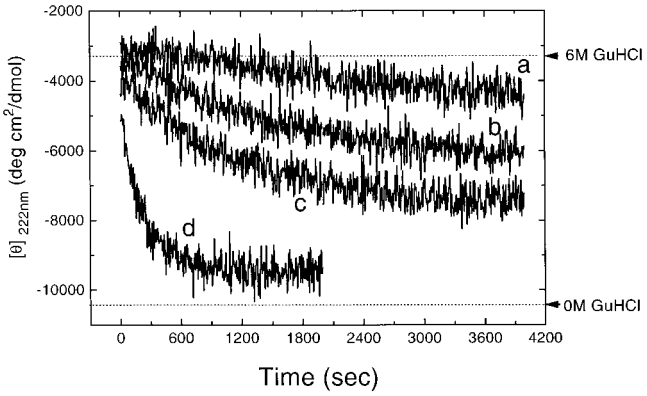

FIGURE 3: Time-dependent changes in CD values at 222 nm for MAP induced by GuHCl concentration jumps from 0 to 3.6−4.0 M at pH 2.9 and 25 °C. Final GuHCl concentrations in 50 mM Gly-HCl buffer were 3.98 (a), 3.95 (b), 3.83 (c), and 3.65 M (d). pH values of sample solutions after measurements were 2.91−2.93. The arrows indicate CD values of the native and denatured states of MAP in 0 and 6.0 M GuHCl at pH 7.0, respectively.

value with time (curve d in Figure 3), suggesting the formation of a secondary structure. The rate of increase in the negative CD value was suppressed by slightly increasing the final GuHCl concentration from 3.65 to 3.98 M, and the constant negative CD values attained after 1 h decreased with an increase in GuHCl concentration as shown in Figure 3(d) to 3(a).

To explore the substance of the strange phenomenon in which the secondary structure increases with the addition of GuHCl, kinetic experiments were performed by slightly changing the pH at a constant concentration of GuHCl. When the final GuHCl concentration slightly decreased to 3.41 M at pH 2.91, the decay curve of CD at 222 nm was similar to that of Figure 3 (d). However, when the pH value slightly increased to 3.31 at the same GuHCl concentration (3.37 M), a rapid decrease in the negative CD value was observed just after mixing MAP with GuHCl with a subsequent change followed by a gradual increase toward a constant value ($-11\,000$ deg cm^2 dmol^{-1}) as shown in Figure 4 (a). This suggests that the secondary structures are newly formed after disruption of the native conformation of MAP. The negative CD value at 222 nm in Figure 4(a) began to increase after about 40 s of mixing, but when the pH value was slightly higher (pH 3.53) at the same concentration of GuHCl (3.41 M), the increment in the negative CD values after unfolding became small as shown in Figure 4(b). Furthermore, at a slightly higher pH of 3.61 at the same concentration of GuHCl (3.40 M), only a monotonic decay curve was observed as shown in Figure 4(c). This decay curve might include two reactions (unfolding from the native state and formation of a secondary structure from the unfolding state), similar to those of Figure 4(a) and 4(b). The rates of unfolding of the native structure and the formation of a new secondary structure were remarkably affected by slight changes in pH and GuHCl concentration.

CD Spectra of MAP in the Presence of Various Concentrations of GuHCl in the Acid Region. As described above, MAP seems to recover the secondary structure after disruption of its native conformation in the presence of about 3 M GuHCl around pH 3. To identify the newly formed structures, the CD spectra of the samples after 1 day incubation in the presence of about 3 M GuHCl in the acid region were

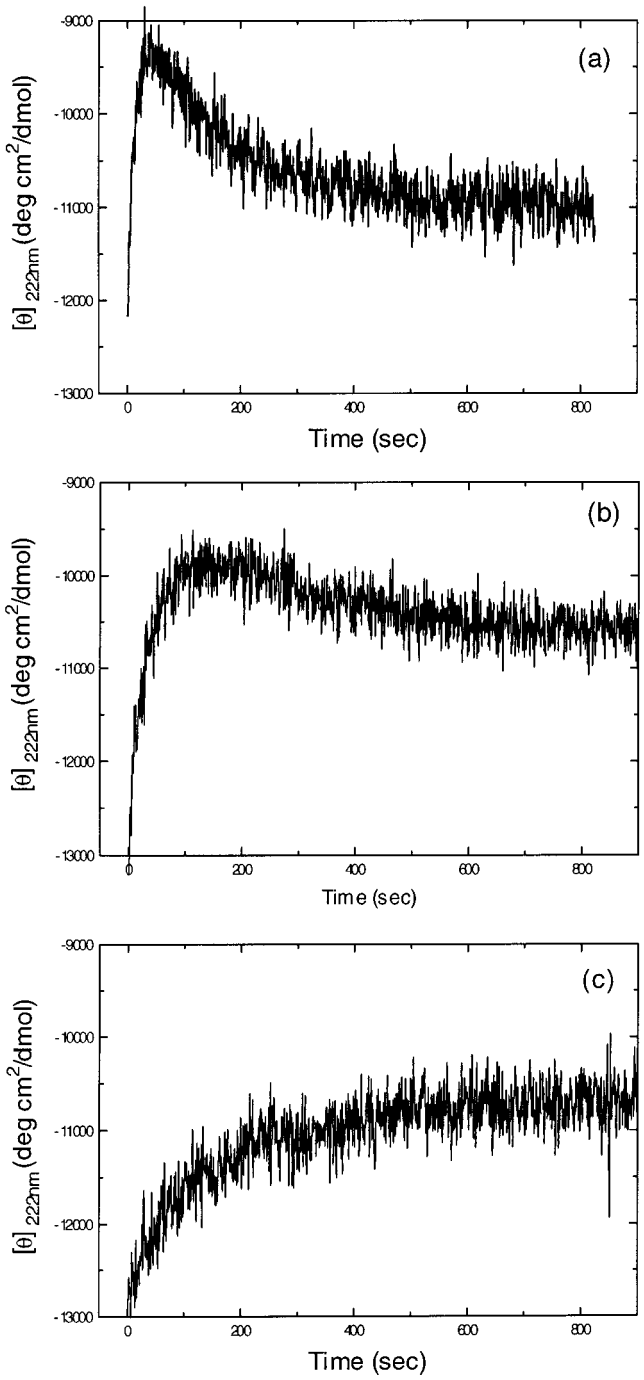

FIGURE 4: Time-dependent changes in CD values at 222 nm for MAP induced by GuHCl concentration jumps to a concentration of 3.4 M at different pHs and 25 °C in 50 mM Gly buffer. (a) GuHCl concentration jumps from 0 to 3.37 M at pH 3.31; (b) GuHCl concentration jumps from 0 to 3.41 M at pH 3.53; (c) GuHCl concentration jumps from 0 to 3.40 M at pH 3.61. The concentrations of GuHCl and pH values were determined after measurements of the time course.

measured in the far-UV region from 205 to 250 nm (Figure 1) and in the near-UV region from 250 to 340 nm (Figure 2) at 25 °C. The CD spectrum of MAP in the presence of 3.27 M GuHCl at pH 2.91 (spectrum b in Figure 1) was clearly different from that in the native state (spectrum c in Figure 1), but similar to that of a β-rich conformation. This indicates that MAP in the presence of 3 M GuHCl near pH 3 changed to a conformation containing a considerable amount of β-sheet from the α-helix-rich content of its native

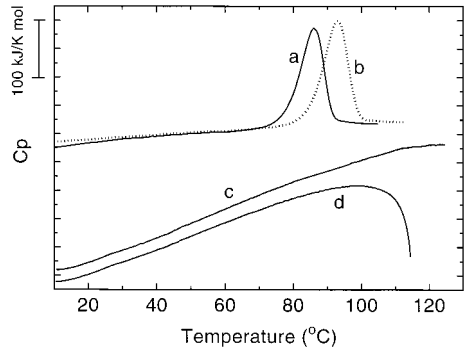

FIGURE 5: Typical endothermic excess heat capacity curves of MAP in the absence and presence of GuHCl at acidic pH. Curves a and b are the DSC curves for MAP in 20 mM Gly-HCl buffer at pH 3.08 and 3.38, respectively; curves c and d, at pH 3.31 and 2.78, respectively, in the presence of 3.30 M GuHCl containing 50 mM Gly-HCl buffer. Concentrations of the proteins were 0.352, 0.455, 0.527, and 0.507 mg/mL for curves a, b, c, and d, respectively. The vertical axes of curves c and d are shifted down to avoid the crossover with curves a and b.

state. From an X-ray structure analysis of MAP, the contents of the α-helix, β-sheet, β-turn, and the remainder are 34, 26, 13, and 27%, respectively (*31*).

On the other hand, the near-UV CD spectrum of MAP in the presence of 3.29 M GuHCl at pH 3.56 [Figure 2(a)] did not have the positive peak at 297 nm characteristic of the native form and was similar to that of denatured MAP under the strong acid conditions (*26*) or in 6 M GuHCl (data not shown).

Calorimetry of MAP in the Acidic Region. The newly formed structure was examined by differential scanning calorimetry (DSC) to test whether heat transition is observed. Around pH 3 in the absence of GuHCl, MAP showed excess heat capacity curves (curves a and b in Figure 5), indicating the existence of a conformation with a cooperative thermal transition. This agrees with the results that the near-UV and far-UV CD spectra near pH 3 are similar to those in the native state at pH 7 (*26*). In the presence of 3.3 M GuHCl at pH 3.3, the DSC curve (curve c in Figure 5) did not show any excess heat capacity up to 125 °C, indicating that the β-rich structure newly formed did not unfold up to that temperature. Furthermore, at a slightly lower pH of 2.8, the heat capacity curve (curve d in Figure 5) suddenly went down near 105 °C. This suggests the appearance of an exothermic reaction, which means that an association (aggregation) reaction (and/or the formation of secondary structures) of the protein began at that temperature. The protein solution for curve d was slightly turbid after heating. The degree of the association (aggregation) depended on pH.

Analytical Ultracentrifugation Experiments with MAP in Various Concentrations of GuHCl. To examine the assembly of MAP in the presence of 3 M GuHCl at pH 3.0, sedimentation equilibrium experiments were performed by analytical ultracentrifugation at 20 °C. As shown in Table 1, the ultracentrifugation analyses indicate that MAP is highly associated in the presence of GuHCl from 1.1 to 4.74 M at pH 3.0, although MAP in 0 and 5.9 M GuHCl is confirmed to be in the monomeric form. In this paper, we call the associated form of MAP containing a considerable content of β-sheet in the presence of about 3 M GuHCl near pH 3.0 the "Am-form of MAP". In these experiments, the Am-form of MAP could apparently reach equilibrium in the ultracen-

Table 1: Apparent Molecular Weight of MAP in Various Concentrations of GuHCl at pH 3.0 and 20 °C

concn of GuHCl (M)	app mol wt
0.00	31K
0.11	125K
1.10	2000K
3.24	1400K
4.74	1800K
5.90	32K

[a] The molecular weight of monomeric MAP from *P. furiosus* is 32 800 (*26*, *28*).

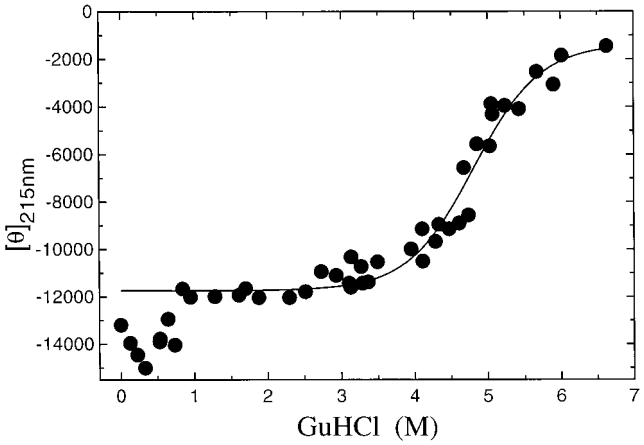

FIGURE 6: GuHCl concentration dependence of CD values at 215 nm for MAP at pH 3.0. The CD values at 215 nm were measured after incubation in various concentrations of GuHCl for 24 h at 25 °C.

trifuge because the protein concentration was not very high (0.5−1.0 mg/mL). When the concentration of MAP increased by more than 10 mg/mL, the Am-form of MAP precipitated as described below.

GuHCl Concentration Dependence of CD Values at 215 nm at pH 3. The DSC curves [Figure 5(c),(d)] for the Am-form of MAP did not show any excess heat capacity up to 100 °C, where MAP is denatured in the absence of GuHCl at the same pH. This suggests that the conformation of the Am-form is not destroyed by heating and is more stable than that in the native state. To examine the stability of the Am-form against a denaturant, GuHCl, the far-UV CD spectra of MAP were measured after 24 h incubation at 25 °C in the presence of various concentrations of GuHCl at pH 3.0. The CD spectra in the presence of GuHCl between 1.0 and 3.5 M were similar to spectrum b in Figure 1, which is characteristic of a β-structure. That is, they show characteristics of the Am-form of MAP. The dependence of CD values at 215 nm on the concentrations of GuHCl showed a sigmoidal curve (Figure 6). This indicates that the conversion from the Am-state to the completely denatured state (D state) of MAP occurs cooperatively; that is, the Am-form of MAP retains the conformation cooperatively disrupted by GuHCl, although the Am-form has no tertiary structure surrounding the aromatic amino acid residues (Figure 2). The midpoint of the transition curve in Figure 6 was 4.82 M GuHCl. Panel a in Figure 4 indicates that the structure in the Am-form is constructed after the native form of MAP is rapidly denatured in the presence of 3.37 M GuHCl at pH 3.31: that is, MAP does not exist as the native state under this condition from an equilibrium point of view. This means that the Am-form of MAP is more stable than the native form, confirming the results of calorimetry.

The CD spectrum in the far-UV region of MAP in 6.6 M GuHCl at pH 3.0 recovered to that of the A-form when the GuHCl concentration was diluted to the pretransition region from 1.0 to 3.0 M. This reveals that the transition between the Am-form and the denatured state is reversible. The conversion from the Am-form to the native state was also reversible, but it took more than 2 weeks in 50 mM Gly buffer at pH 3.0.

The negative CD values at 215 nm increased with increasing GuHCl concentration below 0.5 M (Figure 6). Their CD spectra (data not shown) showed characteristics of an α-helical structure, similar to that of the native MAP. Already at 0.11 M GuHCl, MAP is associated at 4 times the molecular weight of the monomer (Table 1).

The characteristics of the Am-form of MAP are (1) a β-rich structure, (2) no tertiary structure, (3) more stable than the native state toward heating and denaturant, and (4) highly associated forms (accelerated by heating). These features, especially the associated form with the β-structure, are common to amyloid fibrils, suggesting that the Am-form of MAP might be a form of amyloid fibrils. Therefore, we examined whether that is the case.

Tests for Amyloid Fibril Formation of the Am-Form of MAP. CD, ultracentrifugation, and DSC experiments on the Am-form of MAP were performed in clear protein solutions at low protein concentration below 1.3 mg/mL. To test the amyloid fibril formation, MAP solutions in high concentration were prepared. An MAP solution in 50 mM acetate buffer at pH 4.5 was concentrated using a Centricon concentrator 10 (Amicon) up to a protein concentration of 10−20 mg/mL. When the concentrated MAP solution was dialyzed against 50 mM Gly buffer of pH 3.3 containing 3.0 M GuHCl overnight at 4 °C, it became turbid, and MAP precipitated in the dialysis tube. To remove GuHCl from the precipitates (suspension), it was dialyzed against 50 mM Gly buffer of pH 3.3. This freshly prepared suspension was tested by Congo red staining. The suspension was also separated into a supernatant and a precipitate by centrifugation at 13000*g* for electron microscopy experiments.

The dye, Congo red, binds to many amyloid proteins because of their extensive β-sheet structure, and its binding to amyloid fibrils can be judged by a red shift in the spectrum. The maximal peak of the difference spectrum between amyloid fibrils bound with Congo red and the dye-only solution occurs at 541 nm (*30*). The spectrum of the Am-form of MAP showed a red shift in the Congo red solution. A typical difference spectrum between the Am-form of MAP in Congo red solution and dye-only is shown in Figure 7. The peak position is 542.4 nm, close to the value of 541 nm, characteristic of amyloid fibrils, suggesting that the β-structure in the Am-form of MAP is that of amyloid fibrils. Furthermore, a green birefringence was observed between cross-polarizers in the Am-form of MAP stained with Congo red. The development of green birefringence is highly diagnostic for the presence of amyloid (*32*).

X-ray diffraction patterns from the Am-form of MAP were recorded to examine the existence of a cross-β-structure that is typical of amyloid fibrils. A strong reflection at 4.7 Å typical for the cross-β-structure was not found in the diffraction pattern for the prepared sample. Therefore, MAP

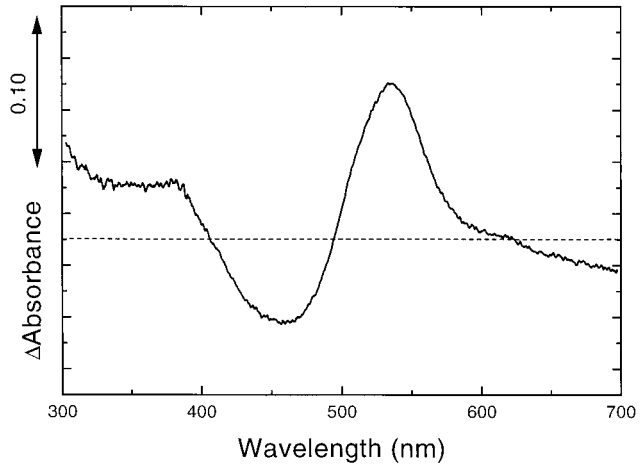

FIGURE 7: Typical difference spectrum between the MAP solution bound with Congo red and dye-only solution. Concentrations of MAP and Congo red were 3.5 and 7.1 μM, respectively. The difference spectrum was corrected by subtracting the spectrum of protein scattering for the suspensions of the Am-form of MAP alone from that of the solution containing the protein and Congo red (*30*).

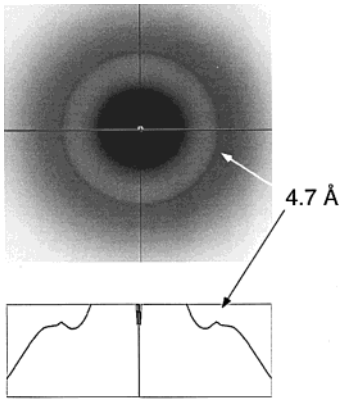

FIGURE 8: X-ray diffraction pattern for the heat-treated Am-form of MAP. The sharp reflection at a spacing of 4.7 Å, which is typical for amyloid fibrils, is marked by arrows. The bottom figure represents the circular averaging from the direct beam point (*47*).

(10−20 mg/mL) in 50 mM Gly buffer at pH 3.3 containing 3.0 M GuHCl was heated at 90 °C for 5 min. After the heat treatment, the sample was exhaustively dialyzed against 20 mM potassium phosphate buffer of pH 7.0, and this material was named the "heat-treated Am-form of MAP". As shown in Figure 8, a sharp reflection clearly appeared at 4.7 Å as a ring. The reflection is ring-shaped because of the lack of preferential fibril orientation within the sample. The 4.7 Å reflection arises from the interstrand spacing between the β-strands in a β-sheet in the direction of hydrogen bonding. A broad intensity maximum should appear around 10 Å in the case of multilayer β-sheet fibrils. In the present case, the peak around 10 Å might be hidden behind a strong background in the central region of the diffraction pattern. The reasons why the heat-treated sample showed a clear reflection at 4.7 Å may be as follows. The association was stimulated by heating, as demonstrated in DSC experiments [Figure 5(d)]. The Am-form of MAP may be acting as the protofilament of amyloid fibrils, and the protofilaments might have grown to form amyloid fibrils due to the heat treatment.

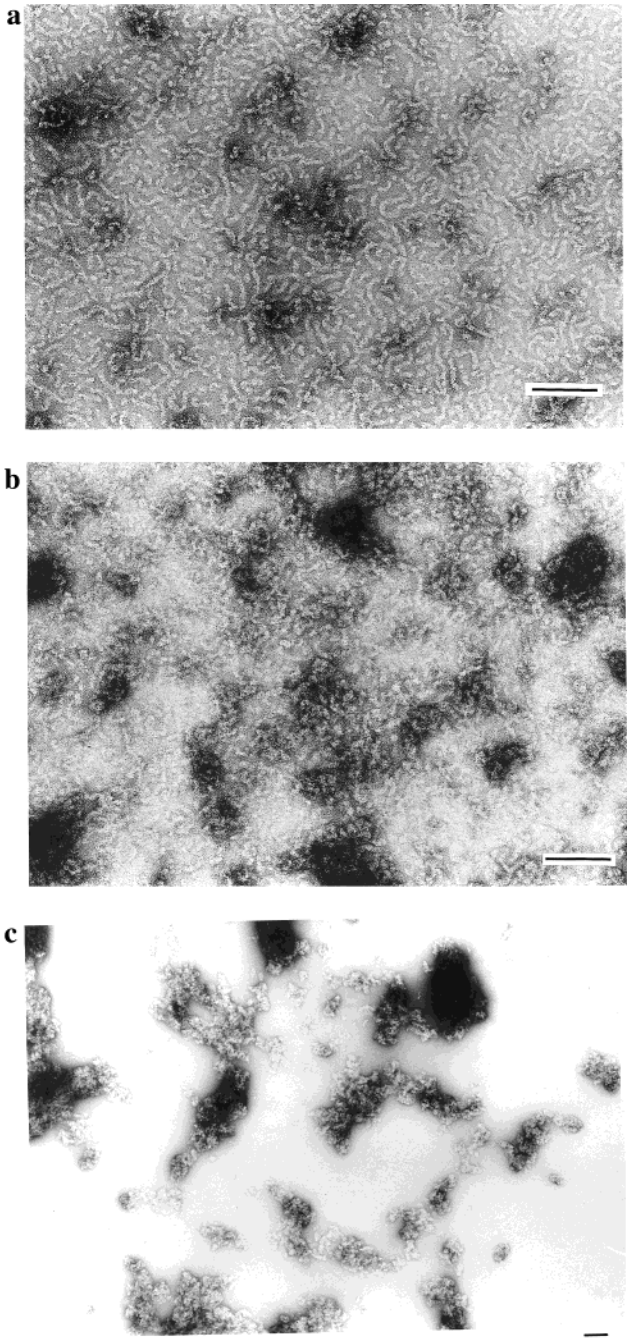

FIGURE 9: Electron micrographs of the negatively stained Am-form of MAP. (a) The supernatant, (b) the precipitates of the Am-form of MAP, and (c) the heat-treated Am-form of MAP. The bar represents 1000 Å.

The fibril formation by the Am-form of MAP was examined by electron microscopy. The precipitates were collected by centrifugation for 30 min at 13000*g* and examined. Figures 9(a) and 9(b) show electron micrographs of the supernatant and precipitates, respectively. Both micrographs show essentially the same features, the image of unbranched fibrils with a length of about 1000 Å and a diameter of 60−80 Å. Under the present condition, long fibrils were not observed. The diameters of the Am-form of MAP are smaller than those of the amyloid fibrils composed of four protofilaments (110−130 Å) (*33, 34*). Recently, Lashuel et al. (*17*) have observed by sedimentation velocity analysis and electron microscopic characterization that an

amyloidogenic protein, a transthyretin mutant (L55P), forms the protofilament of amyloid with a diameter of 47 ± 7 Å under mild conditions. The present micrographs in Figures 9(a) and 9(b) are quite similar to those characterized as the protofilaments (Figure 2 in ref *17*). The precipitates of the Am-form of MAP were dissolved by incubation in 50 mM Gly buffer of pH 3.3 for more than 2 weeks at 4 °C, and the Am-form partly transformed to the native form of MAP as judged by the CD spectrum in the far-UV region. That is, the transition between the Am-form and the native form of MAP is reversible. However, the heat-treated Am-form was not converted back to the native form. Figure 9(c) shows an electron micrograph of the heat-treated Am-form. MAP molecules are highly associated (aggregated), but the extension of the fibrils was not observed by heating in this condition.

DISCUSSION

Amyloid-like Fibril Formation of MAP. To test whether the Am-form of MAP, an associated form containing a considerable content of β-sheet in the presence of 3 M GuHCl near pH 3.0, is amyloid fibrils, the three hallmarks of amyloid were examined: staining with Congo red, a cross-β X-ray diffraction pattern, and a characteristic unbranched fibrillar appearance in the electron micrographs. As described under Results, the Am-form of MAP had the characteristics of amyloid fibrils. The Am-form of MAP in the electron micrograph (Figure 9) was found to be unbranched fibrils with a diameter of about 70 Å characteristic of amyloid fibrils, but the length was not as great. If appropriate conditions are chosen, the length might become greater, like that of typical amyloid fibrils. The size of the Am-form of MAP [Figure 9(a),(b)] is quite similar to the figure characterized as the protofilaments (Figure 2 in ref *17*). Thus, the Am-form might be a prototype of amyloid fibrils.

The reflection at 4.7 Å was clearly observed for the Am-form of MAP after heat treatment, but not for the specimen before the heat treatment. Similar phenomena have been reported for the fibril formation of insulin (*23*). By heating in a water bath to between 80 and 100 °C, insulin, which is a globular protein, polymerizes to form submicroscopic fibrils with the three hallmarks of amyloid. The fibrils can be transformed back to biologically active and crystallizable insulin (*22*). These results suggest that heat treatment stimulates the formation of the cross-β-structure. In the case of MAP, the heat treatment promoted the association and the formation of the β-structure but did not extend the length of the fibrils under the conditions used.

Amyloid-like Fibril Formation of a Highly Stable Protein. A number of studies on amyloidogenic proteins, including transthyretin (*7, 35, 36*) and their mutants (*17, 37, 38*), immunoglobulin light chains (*39, 40*), and human lysozyme mutants (*11, 41, 42*), have been reported. The onset of symptoms caused by amyloid deposition of the transthyretin variants occurs much earlier (*43*), in contrast to late-onset around 80 years of age for amyloid disease from the wild-type transthyretin (*44*). Two kinds of nonconservative single amino acid replacements in human lysozyme are discovered to be capable of forming amyloid fibrils in vivo (*41*), although the wild-type lysozyme appears not to form amyloid fibrils. The differences in the crystal structures and the stabilities between the wild type and mutants of proteins capable of amyloid formation have been examined. The crystal structure of a transthyretin variant, Val30Met, indicates that the overall structure of the tetramer is maintained and slightly rearranged (*45*). Transthyretin amyloid formation requires dissociation to the monomer from the tetramer and subsequent development of an amyloidogenic conformation of the monomer with a partially denatured structure that self-assembles into amyloid (*37, 46*). Transthyretin variants that lead to early onset of amyloid disease destabilize their tetrameric form in favor of the monomeric amyloidogenic intermediate (*37, 38*), indicating that the partially denatured intermediate is critical for the fibril formation and the stability of the tetramer correlates with amyloid formation. In the case of amyloidogenic mutant human lysozymes (*11, 42*), the crystal structure of the mutant lysozyme (Ile56Thr) is also identical to the wild-type one except that the hydroxyl group of the introduced Thr56 forms a hydrogen bond with a water molecule in the interior of the protein (*11*). The physicochemical properties of the mutant protein in the native state are not different from those of the wild-type protein, except that the equilibrium and kinetic stabilities of the mutant protein are remarkably decreased due to the introduction of a polar residue (Thr) in the interior of the molecule. It has been concluded that the amyloid formation of the mutant human lysozyme is due to its stronger conformational tendency toward (partly or/and completely) denatured structures (*11*).

These findings suggest that amyloid formation takes place from structures of partly (or completely) denatured states. If so, would "less stability" be indispensable for amyloid formation? In this paper, we report the amyloid-like fibril formation of the highly stable protein under physiological conditions. Proteins purified from hyperthermophiles, which can grow preferentially at extremely high temperature near the boiling point of water, maximally exhibit their enzymatic activities at those high temperatures and denature at further higher temperatures. The thermostability of MAP from a hyperthermophile, *P. furiosus*, is also extremely high: the denaturation temperature is 106.2 °C at pH 10.2 (*26*). The thermostability of MAP strongly depends on pH. The denaturation temperature was just over 80 °C around pH 3.0 (Figure 5). The stability is still high compared with that of the corresponding proteins from mesophiles.

The Am-form of MAP found in the present study contained a considerable content of the β-sheet structure and was highly associated. The formation of the Am-form of MAP involved destruction of the α-helix followed by consecutive conversion to a β-structure (Figure 4), under considerably extreme conditions such as 3 M GuHCl in the acidic region. This indicates that even highly stable proteins from hyperthermophiles can form amyloid-like fibril under conditions in which the population of (almost completely) denatured states is increased. On the other hand, the DSC curve of the Am-form constructed did not show any excess heat capacity up to 125 °C [Figure 5(c)], indicating that the Am-form of MAP with the β-structure is not unfolded by heating to 125 °C. The association was promoted by heating at a lower pH [Figure 5(d)]. This is consistent with the results in which X-ray diffraction for the Am-form of MAP clearly

showed a peak at 4.7 Å after the heat treatment. The Am-form was cooperatively denatured at higher concentration of GuHCl (Figure 6) than the transition point from the native to the denatured form (Figures 3 and 4), indicating that the Am-form of MAP is more stable compared with the native structure. Therefore, amyloid-like fibrils can be constructed under conditions where the native structure is denatured.

The Mechanism of Amyloid Fibril Formation of MAP. Elucidating the mechanism of amyloid formation should be very important for developing a therapeutic strategy for diseases associated with amyloidosis and also for understanding the mechanism of protein folding. In this paper, we clearly demonstrated that the Am-form of MAP appears after MAP is almost completely denatured as shown in Figure 4(a). This result is not inconsistent with the phenomena observed for amyloidogenic proteins reported by Kelly's group and other groups (*7*, *11*, *16*, *38*, *42*, *46*). Amyloidogenic proteins that have low stability due to mutations would generally be prone to form amyloid, because less stable proteins increase the population of the denatured state in the equilibrium between native (N) and denatured (D) states. We propose the following process for amyloid-like fibril formation of MAP:

$$N \leftrightarrow D \leftrightarrow Ap \rightarrow Af$$

where Ap and Af represents the states in amyloid prototypes (protofilaments) and amyloid-like fibrils, respectively. The process from Ap to Af is irreversible. If the Ap state is more favorable than the D state under appropriate conditions, the reaction proceeds to the Ap state from the D state and finally to the Af state. That is, amyloid-like fibrils accumulate gradually in this irreversible process. The Am-form of MAP (the Ap state) might proceed to amyloid fibrils (the Af state) on heating.

Recently, Dobson's group has proposed that amyloid formation is a common property of globular proteins under appropriate conditions (*24*). Present results confirmed this idea and indicated the following. The amyloid-like form of MAP appears just after the protein is almost completely denatured. Proteins with an inherently high stability such as those isolated from hyperthermophiles can form amyloid-like fibrils under conditions where the D state of a protein is abundantly populated.

REFERENCES

1. Tan, S. Y., and Pepys, M. B. (1994) *Histopathology 25*, 403−414.
2. Carrell, R. W., and Lomas, D. A. (1997) *Lancet 350*, 134−138.
3. Sunde, M., and Blake, C. C. F. (1997) *Adv. Protein Chem. 50*, 123−159.
4. Cohen, A. S., Shirahama, T., and Skinner, K. (1982) in *Electron Microscopy of Proteins 3* (Harris, J. R., Ed.) pp 165−205, Academic Press, London, U.K.
5. Sunde, M., Serpell, L. C., Bartlam, M., Fraser, P. E., Pepys, M. B., and Blake, C. C. F. (1997) *J. Mol. Biol. 273*, 729−739.
6. Pepys, M. W. (1996) in *The Oxford Textbook of Medicine* (Weatherall, D. J., Ledingham, J. G. G., and Warell, D. A., Eds.) 3rd ed., Vol. 2, pp 1512−1524, Oxford University Press, Oxford, U.K.
7. Colon, W., and Kelly, J. W. (1992) *Biochemistry 31*, 8654−8660.
8. Hamilton, J. A., Steinrauf, L. K., Braden, B. C., Liepnieks, L., Benson, M. D., Holmgren, G., Sandgren, O., and Steen, L. (1993) *J. Biol. Chem. 268*, 2416−2424.
9. Schormann, N., Murrell, J. R., Lipenieks, J. J., and Benson, M. D. (1995) *Proc. Natl. Acad. Sci. U.S.A. 92*, 9490−9494.
10. Black, C., and Serpell, L. (1996) *Structure 4*, 989−998.
11. Funahashi, J., Takano, K., Ogasahara, K., Yamagata, Y., and Yutani, K. (1996) *J. Biochem. 120*, 1216−1223.
12. Kelly, J. W. (1996) *Curr. Opin. Struct. Biol. 6*, 11−17.
13. Kelly, J. W. (1997) *Structure 5*, 595−600.
14. Thylen, C., Hammarstrom, S., and Lundgren, E. (1997) *Biochemistry 36*, 5346−5352.
15. Sebastiao, M. P., Saravia, M. J., and Damas, A. M. (1998) *J. Biol. Chem. 273*, 24715−24722.
16. Kelly, J. W. (1998) *Curr. Opin. Struct. Biol. 8*, 101−106.
17. Lashuel, H. A., Lai, Z., and Kelly, J. W. (1998) *Biochemistry 37*, 17851−17864.
18. Lansbury, P. T., Jr. (1999) *Proc. Natl. Acad. Sci. U.S.A. 96*, 3342−3344.
19. Orpiszewski, L., and Benson, M. D. (1999) *J. Mol. Biol. 289*, 413−428.
20. Kocisko, D. A., Priora, S. A., Raymond, G. J., Chesebro, B., Lansbury, P. T., Jr., and Caughey, B. (1995) *Proc. Natl. Acad. Sci. U.S.A. 92*, 3923−3927.
21. Jarrett, J. T., and Lansbury, P. T., Jr. (1992) *Biochemistry 31*, 12345−12352.
22. Waugh, D. F. (1957) *J. Cell. Comp. Physiol. 49*, 145−164.
23. Burke, M. J., and Rougvie, M. A. (1972) *Biochemistry 11*, 2435−2443.
24. Guijarro, J. I., Sunde, M., Jones, J., Cambell, I. D., and Dobson, C. M. (1998) *Proc. Natl. Acad. Sci. U.S.A. 95*, 4224−4228.
25. Chiti, F., Webster, P., Taddei, N., Clark, A., Stefani, M., Ramponi, G., and Dobson, C. M. (1999) *Proc. Natl. Acad. Sci. U.S.A. 96*, 3590−3594.
26. Ogasahara, K., Lapshina, E. A., Sakai, M., Izu, Y., Tsunasawa, S., Kato, I., and Yutani, K. (1998) *Biochemistry 37*, 5939−5946.
27. Ogasahara, K., Nakamura, M., Nakura, S., Tsunasawa, S., Kato, I., Yoshimoto, T., and Yutani, K. (1998) *Biochemistry 37*, 17535−17544.
28. Tsunasawa, S., Izu, Y., Miyagi, M., and Kato, I. (1997) *J. Biochem. 122*, 843−850.
29. Durchschlag, H. (1986) in *Thermodynamic data for Biochemistry and Biotechnology* (Hintz, H.-J., Ed.) Chapter 3, p 45, Springer-Verlag, New York.
30. Klunk, W. E., Jacob, R. F., and Mason, R. P. (1999) *Anal. Biochem. 266*, 66−76.
31. Tahirov, T. H., Oki, H., Tsukihara, T., Ogasahara, K., Yutani, K., Ogata, K., Izu, Y., Tsunasawa, S., and Kato, I. (1998) *J. Mol. Biol. 284*, 101−124.
32. Missmahal, H. P. (1968) in *Amyloidosis* (Mandema, E., Ruinen, L., Scholten, J. H., and Cohen, A. S., Eds.) Excepta Medica, Amsterdam.
33. Serpell, L. C., Sunde, M., Fraser, P. E., Luther, P. K., Morris, E., Sandgren, O., Lundgren, E., and Blake, C. C. F. (1995) *J. Mol. Biol. 254*, 13−118.
34. Blake, C., and Swrpell, L. (1996) *Structure 4*, 989−998.
35. Gustavason, A., Engstrom, U., and Westermark, P. (1991) *Biochem. Biophys. Res. Commun. 175*, 1159−1164.
36. Lai, Z., Colon, W., and Kelly, J. W. (1996) *Biochemistry 35*, 6470−6482.
37. McCutchen, S. L., Colon, W., and Kelly, J. W. (1993) *Biochemistry 32*, 12119−12127.
38. McCutchen, S. L., Lai, Z., Miroy, G., Kelly, J. W., and Colon, W. (1995) *Biochemistry 34*, 13527−13536.
39. Hurle, M. R., Helms, L. R., Li, L., Chan, W., and Wetzel, R. (1994) *Proc. Natl. Acad. Sci. U.S.A. 91*, 5446−5450.
40. Helms, L. R., and Wetzel, R. (1996) *J. Mol. Biol. 257*, 77−86.

41. Pepys, M. B., and Hawkins, P. N. (1993) *Nature 362*, 553−557.
42. Booth, D. R., Sunde, M., Bellotti, V., Robinson, C. V., Hutchinson, W. L., Fraser, P. E., Hawkins, P. N., Dobson, C. M., Radford, S. E., Blake, C. C. G., and Pepys, M. B. (1997) *Nature 385*, 787−793.
43. Saraiva, M. J. M. (1995) *Human Mutat.* 5, 191−196.
44. Gustavsson, A., Jahr, H., Tobiassen, R., Jacobson, D. R., Sletten, K., and Westermark, P. (1995) *Lab. Invest. 73*, 703−708.
45. Terry, C. J., Damas, A. M., Oliviera, P., Saraiva, M. J. M., Alves, A. L., Costa, P. P., Matias, P. M., Sakaki, Y., and Blake, C. C. F. (1993) *EMBO J. 12*, 735−741.
46. Kelly, J. W., Colon, W., Lai, Z., Lashuel, H. A., Mcculloch, J., Mccutchen, S. L., Miroy, G. J., and Peterson, S. A. (1997) *Adv. Protein Chem. 50*, 161−181.
47. Vonderviszt, F., Sonoyama, M., Tasumi, M., and Namba, K. (1992) *Biophys. J. 63*, 1672−1677.

BI991406V